

A multi-grid continuation strategy for parameter-dependent variational inequalities

Ronald H.W. HOPPE

Fachbereich Mathematik, Technische Universität Berlin, D-1000 Berlin 12, Fed. Rep. Germany

Hans D. MITTELMANN*

Department of Mathematics, Arizona State University, Tempe, AZ 85287-1804, U.S.A.

Abstract: For parameter-dependent nonlinear elliptic obstacle problems a path-following multi-grid continuation strategy is developed combining a nested iteration type scheme as predictor with a subsequent multi-grid method as corrector. The performance of the algorithm is illustrated by some numerical results for the Bratu problem.

Keywords: Multi-grid continuation, variational inequalities, obstacle problems, fold points, nonlinear complementarity problems.

1. Introduction

The purpose of this paper is to report on a multi-grid continuation technique for the numerical solution of the following parameter-dependent nonlinear elliptic variational inequality:

Given a bounded domain $\Omega \subset \mathbb{R}^n$, $n \in \mathbb{N}$, and a function $\psi \in L^\infty(\Omega)$, find a pair $(u, \lambda) \in K \times \mathbb{R}^+$, $K = \{v \in H_0^1(\Omega) \mid v \leq \psi \text{ a.e}\}$ such that

$$a(u, v - u) \geq \lambda(f(u), v - u), \quad v \in K \quad (1.1)$$

where $a(u, v) = (\nabla u, \nabla v)$ and $f: \mathbb{R} \rightarrow \mathbb{R}$ is a positive nondecreasing function, (\cdot, \cdot) denoting the usual inner product in $L^2(\Omega)$.

It is well known that in the unconstrained case $K = H_0^1(\Omega)$, where (1.1) reduces to a variational equality, the solution branch, displaying e.g. the energy norm $\sigma = a(u, u)^{1/2}$ in dependence on λ , starts at the origin and first shows increasing σ -values for increasing λ , then has a “left-turning” fold point at some (u_f, λ_f) and finally asymptotically approaches the axis $\lambda = 0$ for $\sigma \rightarrow \infty$. However, in the presence of an obstacle the bifurcation diagram may exhibit a more complicated structure with both “right-turning” and “left-turning” fold points. For the variational inequality branch, which is characterized by a nonempty contact set $B = \{x \in \Omega \mid u(x) = \psi(x)\}$, the behavior of the solution in a vicinity of regular and singular points has been analytically analyzed in [3] using a local parametrization by an arclength-like parameter.

* Supported in part by the Air Force Office of Scientific Research under grant AFOSR-84-0315.

Moreover, the solution has been characterized for the first transition point where B changes from being empty to nontrivial. Computations carried out in [10], using a predictor–corrector continuation strategy, did not only confirm these results numerically but additionally revealed the existence of “right-turning” transition points where λ increases on both sides. The scheme that has been used in [10] is based on a one-parameter Euler type prediction step followed by a corrector chosen as a projected Newton step for the discretized version of the augmented nonlinear system

$$-\Delta u - \lambda f(u) = 0, \quad (1.2)$$

$$\frac{1}{2}(a(u, u) - \sigma^2) = 0, \quad (1.3)$$

in the space of inactive constraints using a most constrained active set strategy.

In this paper, we replace the scalar equation (1.3) by another one which can be deduced from the fact that for sufficiently regular u , ψ the variational inequality (1.1) is equivalent to the nonlinear complementarity problem (cf. e.g. [4])

$$\max(-\Delta u - \lambda f(u), u - \psi) = 0. \quad (1.4)$$

Setting

$$\tilde{a}(u, u) = \int_B |\nabla u|^2 \, dx, \quad \tilde{b}(u) = \int_{\Omega \setminus B} u f(u) \, dx$$

a solution (u, λ) to (1.4) with $a(u, u) = \sigma^2$ obviously satisfies

$$\sigma^2 - (\tilde{a}(u, u) + \lambda \tilde{b}(u)) = 0. \quad (1.5)$$

Note that in contrast to (1.3), as long as $B \subsetneq \Omega$, (1.5) explicitly contains the parameter λ .

The proposed multi-grid continuation strategy which will be explained in detail in the following section uses a nested iteration type scheme for prediction and a multi-grid algorithm as corrector. That multi-grid algorithm performs projected Gauss–Seidel–Newton iteration applied to the discretized complementarity problem (1.4) for fixed λ as a smoother followed by an update of λ according to (1.5) while the defect correction problems on the lower levels are also formulated as complementarity problems augmented by a scalar equation of type (1.5).

2. The multi-grid continuation scheme

In this section, we present a multi-grid continuation method for the numerical solution of the parameter-dependent nonlinear variational inequality (1.1). For notational convenience we will restrict ourselves to the case where Ω is a bounded rectangular domain in \mathbb{R}^2 . We start from a hierarchy $(\Omega_k)_{k=0}^l$ of equidistant grids with step sizes $h_{k+1} = \frac{1}{2}h_k$, $0 \leq k \leq l-1$, given some $h_0 > 0$, and we denote by $u_k = (u_{k,1}, \dots, u_{k,N_k})^T$ and $\psi_k = (\psi_{k,1}, \dots, \psi_{k,N_k})^T$, $N_k = \text{card } \Omega_k$, the vector of unknowns and the vector representing the discrete analogue of the upper obstacle, respectively. Then, if $A_k = (a_{ij}^{(k)})_{i,j=1}^{N_k}$ stands for the matrix associated with the standard five-point approximation of $-\Delta$ with respect to Ω_k and $f_k(u_k)$ is the vector $f_k(u_k) = (f(u_{k,1}), \dots, f(u_{k,N_k}))^T$, the discretized variational inequality (1.1) can be written as the nonlinear complementarity problem

$$\max(G_k(u_k; \lambda_k), u_k - \psi_k) = 0 \quad (2.1)$$

where $G_k(u_k; \lambda_k) = A_k u_k - \lambda_k f_k(u_k)$.

As a continuation parameter we choose the discrete energy norm $\sigma = a_k(u_k, u_k)^{1/2}$ where $a_k(u_k, u_k) = (A_k u_k, u_k)_k$, $(\cdot, \cdot)_k$ denoting the discrete analogue of the L^2 -scalar product with respect to Ω_k . This gives the augmenting equation

$$\frac{1}{2}(a_k(u_k, u_k) - \sigma^2) = 0. \quad (2.2)$$

The extended system (2.1), (2.2) represents a discrete elliptic complementarity problem with an additional scalar equation. Adapting an idea from [5] for discrete parameter-dependent nonlinear elliptic problems to the situation at hand, a possible multi-grid approach is to apply smoothing only in the components of u_k by using e.g. projected Gauss–Seidel–Newton iteration for (2.1) with fixed λ_k . Thus λ_k remains unchanged during the smoothing step and errors in λ_k will be eliminated only by the coarse grid correction.

Instead of using the above approach, we prefer to modify the scalar equation (2.2) in a way which allows to correct λ_k immediately after each smoothing step. As we shall instantly see, that modification is somewhat related to the well-known generalized Rayleigh quotient in the variational equality case: If the pair (u_k, λ_k) solves the extended system (2.1), (2.2) for some given σ_k , then $(A_k u_k)_i = \lambda_k f_{k,i}(u_k)$, $i \in I^1(u_k) = I_k \setminus I_k^2(u_k)$, where $I_k = \{1, \dots, N_k\}$ and $I_k^2(u_k)$ denotes the set of active constraints $I_k^2(u_k) = \{i \in I_k \mid u_{k,i} = \psi_{k,i}\}$. Hence, setting

$$\tilde{a}_k(u_k, u_k) = h_k^2 \sum_{i \in I_k^1} (A_k u_k)_i u_{k,i}, \quad (2.3a)$$

$$\tilde{b}_k(u_k) = h_k^2 \sum_{i \in I_k^1} u_{k,i} f_{k,i}(u_k), \quad (2.3b)$$

obviously $a_k(u_k, u_k) = \tilde{a}_k(u_k, u_k) + \lambda_k \tilde{b}_k(u_k)$, and thus, provided $\tilde{b}_k(u_k) \neq 0$, λ_k satisfies

$$\lambda_k = \Lambda_k(u_k; \sigma_k) := (\sigma_k^2 - \tilde{a}_k(u_k, u_k)) / \tilde{b}_k(u_k). \quad (2.4)$$

Note that $\tilde{b}_k(u_k) > 0$ if $I_k^1(u_k) \neq \emptyset$ and $u_k \in (R^{N_k})^+$, $u_k \neq 0$. Consequently, having computed \tilde{u}_k by smoothing applied to (2.1) with fixed λ_k , as long as $I_k^2(\tilde{u}_k) \subsetneq I_k$, an appropriately updated λ_k -value can be obtained by means of $\tilde{\lambda}_k = \Lambda_k(\tilde{u}_k; \sigma_k)$. The coarse grid correction process is constructed according to Brandt's Full Approximation Scheme (FAS) (cf. e.g. [1]). In particular, computing the defect $d_k^1 = A_k \tilde{u}_k - \tilde{\lambda}_k f_k(\tilde{u}_k)$ with respect to the discrete elliptic equation, the coarse grid correction on the coarser grid Ω_{k-1} involves the complementarity problem

$$\max(G_{k-1}(u_{k-1}; \lambda_{k-1}) - g_{k-1}, u_{k-1} - r_k^{k-1} \psi_k) = 0 \quad (2.5)$$

where

$$g_{k-1} := G_{k-1}(r_k^{k-1} \tilde{u}_k; \tilde{\lambda}_k) - r_k^{k-1} d_k^1 \quad (2.6)$$

and r_k^{k-1} is some appropriately chosen restriction operator.

Denoting by $d_k^2 = \sigma_k^2 - a_k(\tilde{u}_k, \tilde{u}_k)$ the defect with respect to the scalar equation and taking into account the inhomogeneity g_{k-1} in (2.5), the function $\Lambda_{k-1}(\cdot; \cdot)$ has to be modified on level $k-1$ according to

$$\Lambda_{k-1}(u_{k-1}; \sigma_{k-1}) = (\sigma_{k-1}^2 - \tilde{a}_{k-1}(u_{k-1}, u_{k-1}) - \tilde{c}_{k-1}(u_{k-1})) / \tilde{b}_{k-1}(u_{k-1}) \quad (2.7)$$

where

$$\sigma_{k-1}^2 = a_{k-1}(r_k^{k-1} \tilde{u}_k, r_k^{k-1} \tilde{u}_k) + d_k^2,$$

$$\tilde{c}_{k-1}(u_{k-1}) = h_{k-1}^2 \sum_{i \in I_{k-1}^1} u_{k-1,i} g_{k-1,i}.$$

Since projected Gauss–Seidel–Newton iteration is known as an iterative solver for nonlinear complementarity problems, the smoothing process as described above will also be used in the approximate solution of the defect correction process on the coarsest grid Ω_0 . It should be noted that for parameter-independent variational inequalities a corresponding approach has been used by Brandt and Cryer [2] in the linear case and by Hackbusch and Mittelmann [6] in phase I of their two-phase multi-grid algorithm for nonlinear obstacle problems. A special remark must be due to the choice of the restrictions r_k^{k-1} in the fine-to-coarse transfers of the multi-grid cycle. Full weighted restriction cannot be used globally, since otherwise it is not guaranteed that a solution pair (u_1^*, λ_1^*) to (2.1), (2.2) on the finest grid Ω_1 is a fixed point of the multi-grid iteration. Therefore, both in [2] and [6] the use of pointwise restriction is recommended. Also, the result of the defect correction process

$$\tilde{u}_k^{\text{new}} = \tilde{u}_k + p_{k-1}^k (u_{k-1} - r_k^{k-1} \tilde{u}_k)$$

where p_{k-1}^k , $1 \leq k \leq l$, is the usual prolongation based on bilinear interpolation, does not necessarily live in the constraint set which may cause instabilities in particular in a vicinity of the discrete free boundary. For that reason, in [2] and [6] it is suggested to project \tilde{u}_k^{new} onto the constraint set, i.e.

$$\tilde{u}_k^{\text{new}} = \min(\tilde{u}_k + p_{k-1}^k (u_{k-1} - r_k^{k-1} \tilde{u}_k), \psi_k). \quad (2.8)$$

Here, we advocate a slightly different choice of the restriction operators r_k^{k-1} which has been successfully used in [7] and [8] for the numerical solution of free boundary problems by multi-grid techniques. Convergence of the resulting multi-grid scheme can be shown for discrete nonlinear elliptic problems involving M -functions. Taking into account that problems when using full weighted restriction may only occur in the neighborhood of the discrete free boundary, we define r_k^{k-1} locally in the following way:

If $x_i^{(k)} \in \Omega_k$ is the grid point associated to $i \in I_k$, we refer to $B_k^\mu(u_k) = \{x_i^{(k)} \in \Omega_k \mid i \in I_k^\mu(u_k)\}$, $1 \leq \mu \leq 2$, as the set of inactive ($\mu = 1$) and active ($\mu = 2$) grid points. Then, denoting by $N_k(x_i^{(k-1)}) = \{x_i^{(k-1)}, x_i^{(k-1)} \pm h_k e_\mu, 1 \leq \mu \leq 4\} \cap \Omega_k$, where $e_1 = (1, 0)$, $e_2 = (0, 1)$, $e_3 = e_1 + e_2$, $e_4 = e_1 - e_2$, the set consisting of $x_i^{(k-1)}$ and its nearest neighbors in Ω_k , we set

$$(r_k^{k-1} u_k)(x_i^{(k-1)}) = \begin{cases} (\hat{r}_k^{k-1} u_k)(x_i^{(k-1)}) & \text{if } N_k(x_i^{(k-1)}) \cap B_k^\mu(u_k) \neq \emptyset, \quad 1 \leq \mu \leq 2, \\ (\hat{r}_k^{k-1} u_k)(x_i^{(k-1)}) & \text{otherwise,} \end{cases} \quad (2.9)$$

where \hat{r}_k^{k-1} and \hat{r}_k^{k-1} , $1 \leq k \leq l$, stand for full weighted and pointwise restriction, respectively.

Next, we describe a complete multi-grid cycle starting from iterates $u_l = u_l^{(0)}$ and $\lambda_l = \lambda_l^{(0)}$ on the finest grid Ω_l . For that purpose we denote by $(u_k^{(\kappa+1)}, \lambda_k^{(\kappa+1)}) = S_k(u_k^{(\kappa)}, \lambda_k^{(\kappa)}, g_k)$, $\kappa \geq 0$, $0 \leq k \leq l$, the application of a smoothing step consisting of projected Gauss–Seidel–Newton iteration applied to (2.1) for fixed $\lambda_k^{(\kappa)}$

$$u_{k,i}^{(\kappa+1)} = \min \left[u_{k,i}^{(\kappa)} - \left(G_{k,i} \left(\begin{smallmatrix} (i) \\ u_k^{(\kappa)} \end{smallmatrix}; \lambda_k^{(\kappa)} \right) - g_{k,i} \right) / \left(a_{ii}^{(\kappa)} - \lambda_k^{(\kappa)} (\partial f_{k,i} / \partial u_i) \left(\begin{smallmatrix} (i) \\ u_k^{(\kappa)} \end{smallmatrix} \right) \right), \tilde{\psi}_{k,i} \right],$$

$$1 \leq i \leq N_k$$

where

$$\begin{pmatrix} (i) \\ u_k^{(\kappa)} \end{pmatrix} = \left(u_{k,1}^{(\kappa)}, \dots, u_{k,i-1}^{(\kappa)}, u_{k,i}^{(\kappa)}, \dots, u_{k,N_k}^{(\kappa)} \right)^T$$

and

$$\tilde{\psi}_l = \psi_l, \quad \tilde{\psi}_k = r_{k+1}^k \psi_{k+1}, \quad 0 \leq k \leq l-1,$$

followed by a recomputation of λ_k according to

$$\lambda_k^{(\kappa+1)} = \begin{cases} \Lambda_k(u_k^{(\kappa+1)}; \sigma_k) & \text{if } I_k^2(u_k^{(\kappa+1)}) \not\subseteq I_k, \\ \lambda_k^{(\kappa)} & \text{otherwise,} \end{cases}$$

with Λ_k given by (2.4) for $k=l$ and by (2.7) for $0 \leq k \leq l-1$. Note that $g_l=0$ while $g_k, 0 \leq k \leq l-1$, is defined by (2.6).

procedure MGCVI (l, u_l, λ_l, g_l);

integer i, l ; **array** u_l, g_l

if $l=0$ **then**

for $i:=1$ **step** 1 **until** κ_3 **do** (u_l, λ_l) := $S_l(u_l, \lambda_l; g_l)$ **else**

begin **array** u_{l-1}, g_{l-1} ;

for $i:=1$ **step** 1 **until** κ_1 **do** (u_l, λ_l) := $S_l(u_l, \lambda_l; g_l)$;

$u_{l-1} := r_l^{l-1} u_l$;

$\lambda_{l-1} := \lambda_l$;

$g_{l-1} := G_{l-1}(r_l^{l-1} u_l; \lambda_{l-1}) - r_l^{l-1}(G_l(u_l; \lambda_l) - g_l)$;

for $i:=1$ **step** 1 **until** γ_{l-1} **do** MGCVI ($l-1, u_{l-1}, \lambda_{l-1}, g_{l-1}$);

$u_l := \min(u_l + p_{l-1}^l(u_{l-1} - r_l^{l-1} u_l), \tilde{\psi}_l)$;

$\lambda_l := \lambda_{l-1}$;

for $i:=1$ **step** 1 **until** κ_2 **do** (u_l, λ_l) := $S_l(u_l, \lambda_l; g_l)$;

end MGCVI.

It is well known that the performance of path-following continuation methods can be considerably improved by an appropriately chosen predictor. The problem is how to compute predictions $u_i(\sigma'), \lambda_i(\sigma')$ at $\sigma' = \sigma + \Delta\sigma$ on the finest grid Ω_l by efficiently using all available information $u_k(\sigma), \lambda_k(\sigma), 0 \leq k \leq l$, at the preceding parameter value σ . Taking into account that in a multi-grid framework it is advantageous to use smaller continuation steps on the coarser grids (cf. e.g. [5]), a nested iteration type algorithm is suggested which performs $g_k = 2^{l-k}$ continuation steps on levels $0 \leq k \leq l$ with step sizes $(\Delta\sigma)_k = \frac{1}{2}(\Delta\sigma)_{k+1}, 0 \leq k \leq l-1$, given $(\Delta\sigma)_l = \Delta\sigma$. Setting

$$\sigma_k^{(j+1)} = \sigma_k^{(j)} + (\Delta\sigma)_k, \quad 0 \leq j \leq q_k - 1, \quad 0 \leq k \leq l,$$

$$\sigma_k^{(0)} = \sigma, \quad 0 \leq k \leq l,$$

the computation of each pair $(u_k(\sigma_k^{(j+1)}), \lambda_k(\sigma_k^{(j+1)}))$ on level $1 \leq k \leq l$ is preceded by two continuation steps on the lower level $k-1$. In particular, we first provide predictions at $\sigma_k^{(j+1)}$ by

$$u_k(\sigma_k^{(j+1)}) = \min(u_k(\sigma_k^{(j)}) + p_{k-1}^k(u_{k-1}(\sigma_k^{(j+1)}) - u_{k-1}(\sigma_k^{(j)})), \psi_k),$$

$$\lambda_k(\sigma_k^{(j+1)}) = \lambda_k(\sigma_k^{(j)}) + \lambda_{k-1}(\sigma_k^{(j+1)}) - \lambda_{k-1}(\sigma_k^{(j)}), \quad (2.10)$$

on levels $1 \leq k \leq l$ while the Euler predictor from [10] is used on the lowest level $k=0$, and then that prediction step is followed by τ_k applications of the multi-grid algorithm MGCVI (k, u_k, λ_k, g_k) using the predicted values as startiterates.

Note that the Euler predictor from [10] on level $k = 0$ is given by

$$\begin{aligned} u_0(\sigma_0^{(j+1)}) &= u_0(\sigma_0^{(j)}) + \Delta s \dot{u}_0(\sigma_0^{(j)}), \\ \lambda_0(\sigma_0^{(j+1)}) &= \lambda_0(\sigma_0^{(j)}) + \Delta s \dot{\lambda}_0(\sigma_0^{(j)}), \\ \Delta s &= \min\{\overline{\Delta s}, \min\{(\psi_{0,i} - u_{0,i}(\sigma_0^{(j)}))/\dot{u}_{0,i}(\sigma_0^{(j)}), \dot{u}_{0,i}(\sigma_0^{(j)}) > 0, i \in I_0^1(u_0(\sigma_0^{(j)}))\}\}, \\ \|u_0(\sigma_0^{(j)}) + \overline{\Delta s} \dot{u}_0(\sigma_0^{(j)})\| &= \sigma_0^{(j+1)}. \end{aligned}$$

where the pair $(\dot{u}_0, \dot{\lambda}_0)$ with $\dot{u}_0^T \dot{u}_0 + \dot{\lambda}_0^2 = 1$ has to be computed only for the very first continuation step while in the sequel it may be obtained by means of $u_0(\sigma_0^{(j)}) - u_0(\sigma_0^{(j-1)})$ and $\lambda_0(\sigma_0^{(j)}) - \lambda_0(\sigma_0^{(j-1)})$, respectively.

Denoting a formal application of the Euler predictor by $(u_0(\sigma_0^{(j+1)}), \lambda_0(\sigma_0^{(j+1)})) = E_0(u_0(\sigma_0^{(j)}), \lambda_0(\sigma_0^{(j)}))$, the complete nested iteration algorithm can be described as follows:

```

procedure NMGCVI ( $l, u_l, \lambda_l, g_l$ );
integer  $i, j, k, l$ ; array  $u_l, g_l$ 
for  $k := 0$  step 1 until  $l$  do
   $\sigma'_k := \sigma_k + (\Delta\sigma)_k$ ;
  if  $k = 0$  then
     $(u_k(\sigma'_k), \lambda_k(\sigma'_k)) := E_k(u_k(\sigma_k), \lambda_k(\sigma_k))$  else
  begin array  $u_{k-1}$ ;
   $u_k(\sigma'_k) := \min(u_k(\sigma_k) + p_{k-1}^k(u_{k-1}(\sigma'_k) - u_{k-1}(\sigma_k)), \psi_k)$ ;
   $\lambda_k(\sigma'_k) := \lambda_k(\sigma_k) + \lambda_{k-1}(\sigma'_k) - \lambda_{k-1}(\sigma_k)$ ;
  for  $i := 1$  step 1 until  $\tau_k$  do MGCVI ( $k, u_k, \lambda_k, g_k$ );
  if  $k = 1$  go to end NMGCVI else
   $\sigma_k := \sigma'_k$ ;
  for  $j := 0$  step 1 until  $k$  do NMGCVI ( $j, u_j, \lambda_j, g_j$ );
end NMGCVI.

```

3. Numerical results

For the Bratu problem, i.e., $f(x) = \exp(x)$, $x \in \mathbb{R}$, in (1.1), considered on the unit square $\Omega = (0, 1) \times (0, 1)$, and constant as well as variable upper obstacles we have performed several computations for different grid hierarchies $(\Omega_k)_{k=0}^l$ with the equidistant grid Ω_0 of step size $h_0 = \frac{1}{4}$ as the coarsest grid. The continuation was started at a point of the variational equality branch choosing $(\Delta\sigma)_1 = 0.2$ as continuation step on the finest grid with the optional choice of lower continuation steps in the vicinity of critical points or if convergence does not occur. As multi-grid parameters we have chosen $\gamma_k = 2$, $1 \leq k \leq l-1$ (“W-cycle”) with $\kappa_1 = 2$ pre-smoothing and $\kappa_2 = 2$ post-smoothing steps, while the number of iterations for the solution of the defect correction on the coarsest grid was limited by $\kappa_3 = 20$. In NMGCVI we have taken $\tau_k = 1$, $1 \leq k \leq l \leq 1$, i.e., we only executed one multi-grid cycle at each intermediate level in the nested iteration procedure.

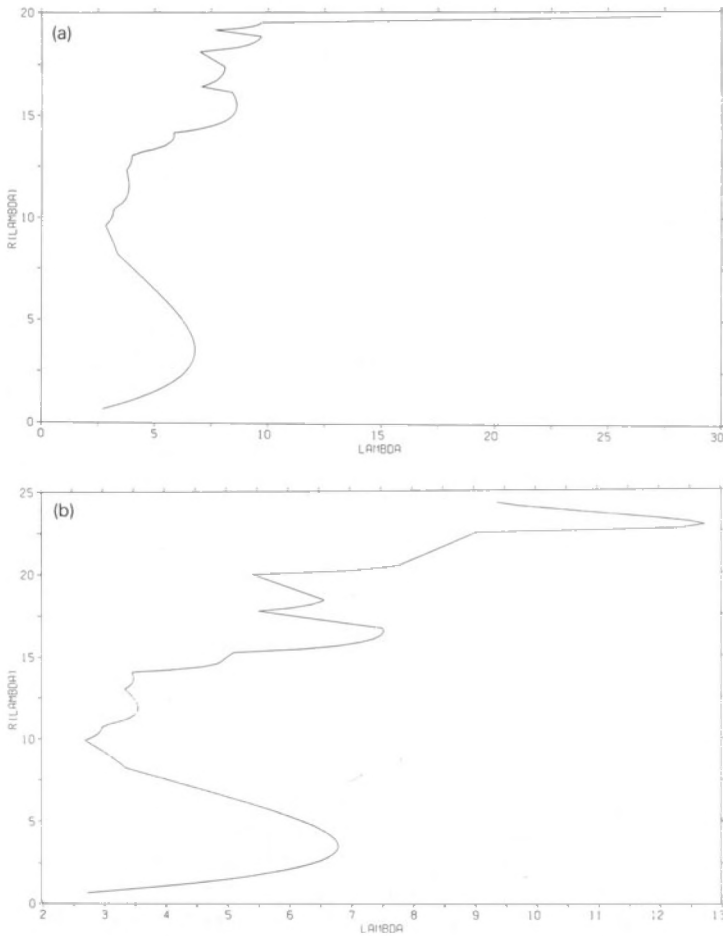


Fig. 1. (a) Constant obstacle, $C = 2.0$. (b) Constant obstacle, $C = 4.0$.

Numerical results have been obtained for $1 \leq l \leq 4$, i.e., a maximal number of five grids with finest step size $h_4 = \frac{1}{64}$ have been used, but for the sake of better visibility of the effects plots displaying the solution branch over the full range of activation levels from $B_l^2 = \emptyset$ up to $B_l^2 = \Omega_l$ are only given for $l = 1$ and $l = 2$.

For $l = 2$, Figs. 1(a) and (b) show the solution branch in case of constant obstacles $\psi \equiv C = 2.0$ and $\psi \equiv C = 4.0$, respectively, while Tables 1(a) and (b) contain the corresponding values of σ , λ and the number of active grid points (NAGP). In case $C = 2.0$, apparently there are no fold points but for $C = 4.0$ the results are quite different. A typical situation on the variational inequality branch is the occurrence of a transition point, where λ increases on both sides,

followed by a “left-turning” fold point (cf. e.g. the situation where NAGP changes from 1 to 5, 5 to 9, 109 to 117 and 165 to 169 in Table 1(b)).

As variable obstacles we have taken upper obstacles of the form $\psi(x) = A + B[(x - 0.5)^2 + (y - 0.5)^2]^{1/2}$, $x \in \Omega$. In case $l = 1$, Figs. 2(a) and (c) display the solution branch for $A = 4.0$, $B = -1.0$ (concave obstacle) and $A = 4.0$, $B = +1.0$ (convex obstacle) while for reference Fig. 2(b) gives the solution branch in the constant obstacle case $A = 4.0$, $B = 0.0$. Obviously, there is a different behavior when the obstacle changes from being concave to convex. This is supported by Table 2 which, for $l = 2$, contains the σ , λ -values in the range from NAGP = 109 to NAGP = 121. For the concave obstacle there are only regular transition points and no fold points while in the convex case there is a regular transition point followed by a “left-turning” fold point and a transition point with increasing λ -values on both sides of it.

Further, in case of the constant obstacle $\psi \equiv C = 4.0$ we have tested the performance of the multi-grid algorithm MGCVI by computing asymptotic convergence rates $\gamma_l^{\text{MG}}(\sigma_l)$ which relate the gain in accuracy to the amount of work for implementation. As work unit we have taken one projected Gauss–Seidel–Newton iteration on the finest grid Ω_l . Then, denoting by N_{WU} the number of work units required for the execution of one multi-grid cycle and by $\|e_l^r(\sigma_l)\|_{l,2}$ the

Table 1(a)

σ	λ	NAGP	σ	λ	NAGP
0.5894	2.5606	0	8.4144	17.5232	101
1.5894	5.3183	0	8.6144	18.8233	109
2.5894	6.5671	0	9.0144	21.7028	117
2.9894	6.7536	0	9.6144	25.9402	117
3.3894	6.8013	0	9.9144	26.8974	117
3.7894	6.7339	0	10.0144	27.8094	121
4.5894	6.3368	0	10.4144	29.7935	133
4.6019	6.3373	1	10.6144	31.7721	149
4.7519	6.3637	1	10.8144	34.0120	157
4.7644	6.3748	5	11.2144	40.3412	165
4.9394	6.5605	5	11.8144	52.2702	165
4.9644	6.5898	9	12.0144	54.7237	165
5.2144	6.8927	9	12.2144	57.4017	169
5.2644	6.9532	13	12.8144	63.6501	169
5.3644	7.1191	13	13.2144	66.2830	169
5.4144	7.2155	21	13.8144	68.7724	169
5.7144	7.8242	21	14.2144	69.7008	169
5.8144	8.0057	25	14.4144	69.9801	169
6.0144	8.4418	29	14.5058	70.0688	169
6.2144	9.0269	37	15.2574	75.6122	205
6.4144	9.6173	45	15.4574	78.7991	205
6.8144	10.6653	45	15.6574	84.3669	213
7.0144	11.4456	61	15.8574	89.6733	213
7.2144	12.3035	69	16.0574	101.6607	221
7.61447	14.0487	77	16.2574	132.0260	221
8.0144	15.5846	77	16.4574	138.2963	221
8.2144	16.2825	93	16.6574	138.5833	225

Table 1(b)

σ	λ	NAGP	σ	λ	NAGP
0.5894	2.5606	0	15.9267	6.2794	101
1.5894	5.3183	0	16.5167	7.2596	109
2.5894	6.5671	0	17.3167	8.5033	117
2.9894	6.7536	0	18.3167	9.5763	117
3.3894	6.8013	0	18.5167	9.5976	117
3.7894	6.7339	0	18.7824	9.5550	117
4.7894	6.1962	0	18.8824	9.5208	121
5.7894	5.3413	0	19.8824	10.1562	141
7.8542	3.3532	0	20.2824	10.7251	149
8.0042	3.2230	1	21.0824	13.1735	157
8.4542	3.0104	1	21.6824	14.4434	165
8.4667	3.0108	5	21.8824	17.4803	165
8.6417	3.0155	5	22.0824	19.0613	165
8.8417	3.0037	5	22.2824	19.6475	165
8.9417	2.9960	9	22.4824	18.9057	169
9.1417	3.0135	9	22.6824	21.3900	169
9.5417	2.9947	9	23.6824	25.7265	169
9.6417	2.9884	13	24.0824	25.9195	169
9.9417	3.0369	13	24.1824	25.8786	169
9.9617	3.0484	21	24.4449	25.5680	169
10.7167	3.2563	21	24.4925	25.4703	169
10.8167	3.2693	25	25.7441	22.1109	181
11.0167	3.3019	25	26.2191	23.2224	181
11.0667	3.3227	29	26.8191	20.7140	189
11.2667	3.4030	29	27.3886	23.5540	189
11.3167	3.4337	37	27.9902	19.5484	197
12.0167	3.8103	45	28.5152	24.3515	197
12.6167	4.0538	45	29.2152	19.6577	205
12.8167	4.0936	49	29.6347	26.3247	205
13.0167	4.1660	49	30.4863	20.1527	213
13.2167	4.3796	61	30.8355	31.3168	213
13.6167	4.7375	69	31.9370	19.8684	221
14.3167	5.1790	69	32.1370	50.4002	221
14.4167	5.3608	77	32.3370	50.0846	221
15.0167	5.6869	77	32.7370	43.1378	221
15.2167	5.7431	81	33.1370	37.5104	225

discrete L_2 -norm of the difference $e_l^{\nu}(\sigma_l) = u_l^{\nu}(\sigma_l) - u_l^{\nu-1}(\sigma_l)$, $\nu \geq 1$, of two subsequent iterates, $\gamma_l^{\text{MG}}(\sigma_l)$ has been determined according to

$$\gamma_l^{\text{MG}}(\sigma_l) = (\|e_l^{\nu^*}(\sigma_l)\|_{l,2} / \|e_l^1(\sigma_l)\|_{l,2}) ** (1 / [(\nu^* - 1) * N_{\text{wU}}])$$

where $\nu^* > 1$ is the iterate for which either machine accuracy has been reached or the total number of work units has exceeded 100. We have compared $\gamma_l^{\text{MG}}(\sigma_l)$ for σ_l -values ranging over the whole interval $[\sigma_l^{\min}, \sigma_l^{\max}]$ observing no significantly different behaviour on the different parts of the solution branch, i.e., for different values of NAGP. As mean values $\tilde{\gamma}_l^{\text{MG}}$, averaged with respect to σ_l , we have obtained $\tilde{\gamma}_l^{\text{MG}} = 0.60$ for $l = 3$ and $\tilde{\gamma}_l^{\text{MG}} = 0.62$ for $l = 4$. Note that these asymptotic convergence rates are almost in the same range as those obtained for multi-grid

algorithms applied to other types of free boundary problems (cf. e.g. [2], [8]). We have also computed convergence rates $\gamma_l^{\text{SG}}(\sigma_l)$ and $\tilde{\gamma}_l^{\text{SG}}$ for the solution of (2.1) with augmenting equation (2.4) on the single grid Ω_l by projected SOR-Newton iteration with suboptimal relaxation parameter. The results were $\tilde{\gamma}_l^{\text{SG}} = 0.84$ for $l = 3$ and $\tilde{\gamma}_l^{\text{SG}} = 0.95$ for $l = 4$ thus reflecting the expected asymptotic convergence rate $O(1 - h_l^2)$ for that single-grid iteration scheme.

Finally, for comparison with different (single-grid) continuation strategies applied to the same problem the reader is referred to [9] and [10].

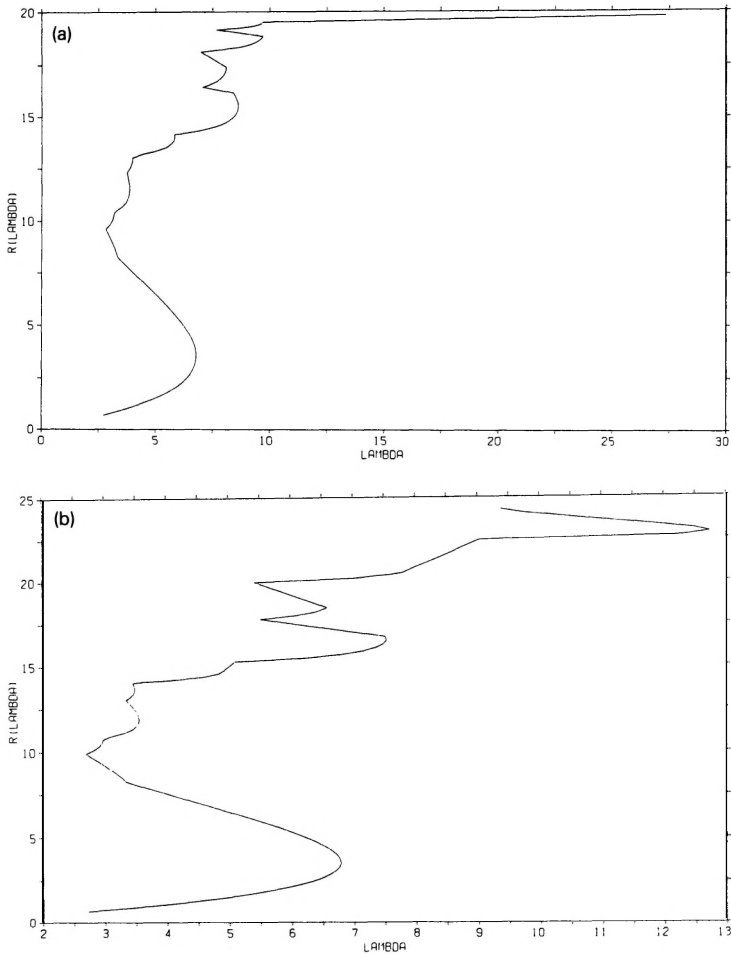


Fig. 2. (a) Variable obstacle, $A = 4.0$, $B = -1.0$. (b) Constant obstacle, $C = 4.0$. (c) Variable obstacle, $A = 4.0$, $B = 1.0$.

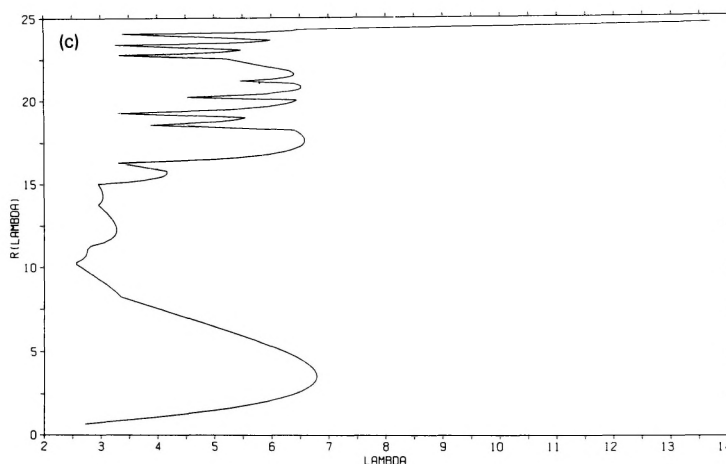


Fig. 2 (continued).

Table 2

NAGP	$A = 4.0, B = -1.0$		$A = 4.0, B = 0.0$		$A = 4.0, B = 1.0$	
	σ	λ	σ	λ	σ	λ
109	15.56	9.66	17.12	8.07	18.41	6.47
117	15.76	9.98	17.32	8.50	18.61	6.54
117	16.30	11.26	18.52	9.60	19.98	7.76
117	17.10	11.83	18.78	9.55	20.33	7.67
121	17.30	11.91	18.88	9.52	20.53	7.56
121	17.40	11.96	19.08	9.61	20.68	7.59

References

- [1] A. Brandt, Multi-level adaptive solutions to boundary-value problems, *Math. Comp.* **31** (1977) 333–390.
- [2] A. Brandt and C.W. Cryer, Multi-grid algorithms for the solution of linear complementarity problems arising from free boundary problems, *SIAM J. Sci. Stat. Comput.* **4** (1983) 655–684.
- [3] F. Conrad, F. Issard-Roch, C.-M. Brauner and B. Nicolaenko, Nonlinear eigenvalue problems in elliptic variational inequalities: A local study, *Comm. Partial Differential Equations* **10** (1985) 151–190.
- [4] R. Glowinski, J.L. Lions and R. Trémolières, *Numerical Analysis of Variational Inequalities* (North-Holland, Amsterdam, 1981).
- [5] W. Hackbusch, Multi-grid solution of continuation problems, in: R. Ansorge, T. Meis and W. Törnig, Eds., *Iterative Solution of Nonlinear Systems*, Lecture Notes in Math. **953** (Springer, Berlin, 1982).
- [6] W. Hackbusch and H.D. Mittelmann, On multi-grid methods for variational inequalities, *Numer. Math.* **49** (1983) 239–254.
- [7] R.H.W. Hoppe, On the numerical solution of variational inequalities by multi-grid techniques, in: B. Karasözen et al., Eds., *Proc. Internat. Symp. on Numerical Analysis*, Ankara, Turkey, September 1987 (Plenum Press, New York, to appear).

- [8] R.H.W. Hoppe and R. Kornhuber, Multi-grid solution of the two-phase Stefan problem, in: S. McCormick, Ed., *Proc. 3rd Copper Mountain Confer. on Multigrid Methods*, Copper Mountain, Colorado, April 6–10, 1987 (Marcel Dekker, New York, 1988).
- [9] E. Miersemann and H.D. Mittelmann, Continuation for parametrized nonlinear variational inequalities, *J. Comput. Appl. Math.* **26** (1&2) (1989) 23–34 (this issue).
- [10] H.D. Mittelmann, On continuation for variational inequalities, *SIAM J. Numer. Anal.* **24** (1987) 1374–1381.